European Journal of Radiology Open 5 (2018) 52–57

Contents lists available at ScienceDirect

European Journal of Radiology Open

journal homepage: www.elsevier.com/locate/ejro

# Characterization of diffuse orbital mass using Apparent diffusion coefficient in 3-tesla MRI

Sahar M. ElKhamary[a,*], Alicia Galindo-Ferreiro[b], Laila AlGhafri[b], Rajiv Khandekar[c], Silvana Artioli Schellini[b]

[a] Diagnostic Imaging Department, King Khaled Eye Specialist Hospital, Riyadh, Saudi Arabia
[b] Oculoplastic Division, King Khaled Eye Specialist Hospital, Riyadh, Saudi Arabia
[c] Research Department, King Khaled Eye Specialist Hospital, Riyadh, Saudi Arabia

ARTICLE INFO

*Keywords:*
MRI
ADC
Diffusion
Diffuse
Orbital
Mass

ABSTRACT

*Purpose:* To evaluate if the apparent diffusion coefficient (ADC) value in diffusion-weighted magnetic resonance imaging (DW-MRI) improves the diagnostic accuracy of diffuse orbital masses.

*Materials and methods:* ADC DW-MRI was used to evaluate cases of diffuse orbital masses at our institution from 2000 to 2015. Lesions were grouped according to histopathologic diagnosis as, benign, pre-malignant and malignant. Lymphoproliferative lesions were further subgrouped as lymphoma or other lymphoproliferative lesions. The validity of the ADC value for the diffuse orbital mass was compared between groups. The area under curve (AUC) was also calculated.

*Results:* Thirty-nine cases of diffuse orbital masses were evaluated. The median ADC was 0.58 (25% quartile 0.48; minimum: 0.45; maximum: $1.72 \times 10^{(-3)}$) for the malignant tumors and 1.19 (25% quartile 0.7; minimum: 0.5; maximum: $1.95 \times 10^{(-3)}\,mm^{(2)}\,s^{(-1)}$) for benign lesions. This difference in ADC between lesions was statistically significant (Mann Whitney *U* test $P < 0.001$). The median ADC was 0.51 (25% quartile 0.48) for lymphomas and 0.9 (25% quartile 0.7) for other lymphoproliferative lesions. This difference in ADC was statistically significant (Mann Whitney *U* test $P = 0.02$). An ADC value of $0.8 \times 10^{(-3)}\,mm^{(2)}\,s^{(-1)}$ was noted as the ideal threshold value for differentiating malignant from benign diffuse orbital masses. The validity of ADC in predicting a malignant or benign diffuse orbital mass had a sensitivity of 87%, specificity of 67% and accuracy of 88%.

*Conclusion:* ADC is a promising imaging metric to characterize malignant and benign diffuse orbital masses and to distinguish lymphomas from other non−lymphoproliferative lesions.

## Advances in knowledge

- We have used the apparent diffusion coefficient (ADC) value in diffusion-weighted magnetic resonance imaging (DW-MRI) to evaluate diffuse orbital masses with histopathology-proven diagnosis.
- We have used the ADC to show that different types of diffuse orbital lesions may be distinguished based on value. A threshold value is presented for malignant versus benign diffuse lesions.

## Implication(s) for patient care

- Our approach allows non-invasive diagnosis of patients where the location of the lesion precludes an orbital biopsy and can give some clues about possible malignacies.
- As a threshold value is determined in this study, patients may be diagnosed earlier and undergo treatment earlier.

## Summary statement

The apparent diffusion coefficient (ADC) value in diffusion-weighted magnetic resonance imaging (DW-MRI) of diffuse orbital masses shows good sensitivity in differentiating malignant from benign lesions and to distinguish lymphomas from non-lymphoproliferative lesions.

## 1. Introduction

Diffuse orbital masses include a heterogeneous group of diseases

* Corresponding author: Diagnostic Imaging Department, King Khaled Eye Specialist Hospital, Riyadh, Saudi Arabia.
*E-mail addresses:* skhamary@kkesh.med.sa (S.M. ElKhamary), agalindo@kkesh.med.sa (A. Galindo-Ferreiro), lghafari@kkesh.med.sa (L. AlGhafri), rkhandekar@kkesh.med.sa (R. Khandekar), sartioli@fmb.unesp.br (S.A. Schellini).

https://doi.org/10.1016/j.ejro.2018.03.001
Received 28 November 2017; Received in revised form 2 March 2018; Accepted 11 March 2018
Available online 26 March 2018

with considerable overlap in clinical findings that warrant appropriate tools for the correct diagnosis. Conventional magnetic resonance image (MRI) including the contrast-enhanced method is a very useful non-invasive method for the differential diagnosis, prediction and management of orbital masses [1–5].

Diffusion- weighted magnetic resonance imaging (DW-MRI) was introduced in 1986. DW-MRI is an excellent diagnostic modality to differentiate between benign and malignant tumors of brain, parotid, head and neck, cervical lymph and thyroid nodules [6,7] and to better define orbital masses [5–8].

Non-invasive imaging methods are helpful in differentiating between benign and malignant diffuse orbital masses from inflammatory processes. However, studies are rare on the use of DW-MRI to characterize orbital masses and its role is not clearly defined [1,3,9,10]. The apparent diffusion coefficient (ADC) from DW-MRI can be used to better characterize some lesions. However, threshold ADC values that may differentiate specific orbital lesions require clarification.

In this study, we evaluate the role of the ADC component of DW-MRI images in the diagnosis of diffuse orbital masses that were confirmed by histopathology. We also evaluated the utility of ADC DW-MRI as a metric to increase the accuracy of diagnosing diffuse orbital lesions.

## 2. Methods

This retrospective study evaluated patients with diffuse orbital lesions who presented to our institution, from 2000 to 2015. The institutional ethics committee board approved the study protocol and informed consent was waived due to the retrospective nature of the study.

Cases were included if they had a provisional diagnosis of diffuse orbital mass (unilateral or bilateral) that underwent DW-MRI of the orbit and had undergone a histopathology evaluation. Exclusion criteria were, a history of previous treatment or surgery and lack of a histopathologic confirmation of the diagnosis.

### 2.1. Diffuse orbital mass classification

Lesions were grouped according the histopathologic characteristics into: [1] *benign lesions* (sarcoidosis, amyloidosis, *angiolymphoid hyperplasia with eosinophilia*, Kimura, idiopathic, myositis, Ig G4 orbital disease, plexiform neurofibroma), [2] *pre-malignant* (*Castleman* disease, benign lymphoid hyperplasia, atypical lymphoid hyperplasia) and [3] *malignant lesions* (lymphoma, leukemia, metastatic tumors). The lymphoproliferative lesions were sub-grouped as lymphoma and other lymphoproliferative lesions (*Castleman* disease, benign lymphoid hyperplasia, atypical lymphoid hyperplasia) (Figs. 1 and 2).

### 2.2. MRI and DW-MRI technique

The imaging studies were performed with a 3-T scanner (Magnetom Allegra; Siemens, Erlangen, Germany) with a dedicated head coil. The gradient strength was 40 mT/m and the slew rate was 400 T/m/s. First, sagittal then coronal spin-echo T1 DW-MRI scans were obtained with TR/TE of 450–750/9–13 ms. Axial and coronal T2 DW-MRI scans were obtained with TR/TE of 2400–2800/19–96 ms, FOV of 20 × 22 cm, section thickness of 4 mm, interslice gap of 1–2 mm and matrix of 320 × 320. All patients had additional high resolution three-dimensional constructive interference in steady state sequences (CISS sequence) with the following parameters: repetition time (TR) of 10.76 ms, time echo (TE) of 5.38 MS, 70° flip angle, 200 × 200 mm field of view (FOV), 512 × 512 mm matrix, and 64 slices and 0 slice gap.

Axial, sagittal and coronal post-contrast T1-DW-MRI with fat suppression was performed with a frequency-selective pre-saturation pulse using intravenous injection of 0.1 mmol/kg Gadopentate dimeglumine (Magnevist; Schering, Berlin, Germany), (TR/TE = 400–575/13–15 ms) for all patients.

DW-MRI was obtained in the axial plane using a multi-slice spin echo planar imaging (EPI) sequence. Imaging parameters were as follows: TR/TE of 3200/81 ms, FOV of 20 × 22 cm, section thickness of 4.0 mm, interslice gap of 1.0–2.0 mm, number of excitations of 6, matrix of 128 × 128, EPI factor of 128 and RF pulse bandwidth of 1200. Diffusion-probing gradients were applied in the three orthogonal directions ($x$, $y$ and $z$) with the same strength. DW-MRI was acquired with diffusion-weighted b factor, of 0500 and 1000 s/mm$^2$, and ADC maps were generated for all images. The data acquisition time for the DW-MRI was 1.33 min.

Region of interest (ROI) analysis was performed by using measurements of the areas of abnormality seen on conventional MRI sequences. To achieve standardized conditions for result analysis and avoid data contamination from adjacent structures, 2 ROIs placed within a given area of the solid region were taken. The pre-contrast and post-contrast spin-echo MRI images were obtained in this manner and provided for review without information about the final clinical and pathological diagnosis. Distortion artifacts were carefully excluded from the ROI delimitation, avoiding the cystic regions as much as possible to avoid a falsely elevated ADC value. We obtained averaged ADC values of 2 ROIs. A commercial workstation (Syngo's Siemens Medical Solutions, Erlangen, Germany) was used for pixel-based ADC maps.

### 2.3. Statistical analysis

Data was collected on an Excel spreadsheet (Microsoft Corp., Redmond, WA, USA) and subsequently transferred into a Statistical Package for Social Sciences spreadsheet (SPSS-23) (IBM Corp., Armonk, NY, USA). The Mann Whitney $U$ test was used to compare ADC values between malignant, premalignant and benign orbital lesions. The ADC values of lymphoproliferative and non-lymphoproliferative lesions were also compared with the Mann Whitney $U$ test. A two-sided $P$ value derived from the Kruskal-Wallis test was used to test statistical significance. A $P$ value less than 0.05 was considered statistically significant. The ADC value was estimated for each subgroup for comparison. The receiver operating characteristic curve was plotted to determine the area under curve (AUC) using SPSS 23.

## 3. Results

The study sample was comprised of 39 patients with diffuse orbital mass, with a median age of 40.6 ± 18.8 years. There 59% females and 41% males in the study sample. Thirty-two (82.1%) patients had a lesion in one orbit only. There were malignant lesions in 15 (38.5%) patients, pre-malignancies in 2 (5.1%) and benign lesions in 22 (56.4%) patients. Incisional biopsy was performed in 31 (79.5%) patients and excisional biopsy in 8 (20.5%) patients.

The median ADC of the malignant lesion was 0.58 (25% quartile 0.48; minimum 0.45; maximum 0.72). The median ADC of pre-malign lesions was 0.83 (25% quartile 0.7; minimum 0.7; maximum 0.92). The median ADC of benign lesions was 1.19 (25% quartile 0.7; minimum 0.5; maximum 1.95) (Table 1). The comparisons of ADC values of benign and malignant lesions are graphically represented in Fig. 3. There was a statistically significant difference in ADC between malignant and benign lesions (Mann Whitney $U$ test $P < 0.001$).

The median ADC for lymphomas was 0.51 (25% quartile 0.48; minimum 0.45; maximum 0.6) while for other lymphoproliferative lesions was 0.9 (25% quartile 0.7; minimum 0.5; maximum 1.72) (Table 1). There was a statistically significant difference in ADC values between lymphoma and other lymphoproliferative lesions (Mann Whitney $P = 0.02$) and this is graphically presented in Fig. 3.

When an ADC value of $0.8 \times 10^{(-3)}\,mm^{(2)}\,s^{(-1)}$ was used as a threshold value for differentiating malignant from benign diffuse orbital mass, the best validity results were obtained, with a sensitivity of 86.7%, specificity of 66.9%, positive predictive value of 61.9% and

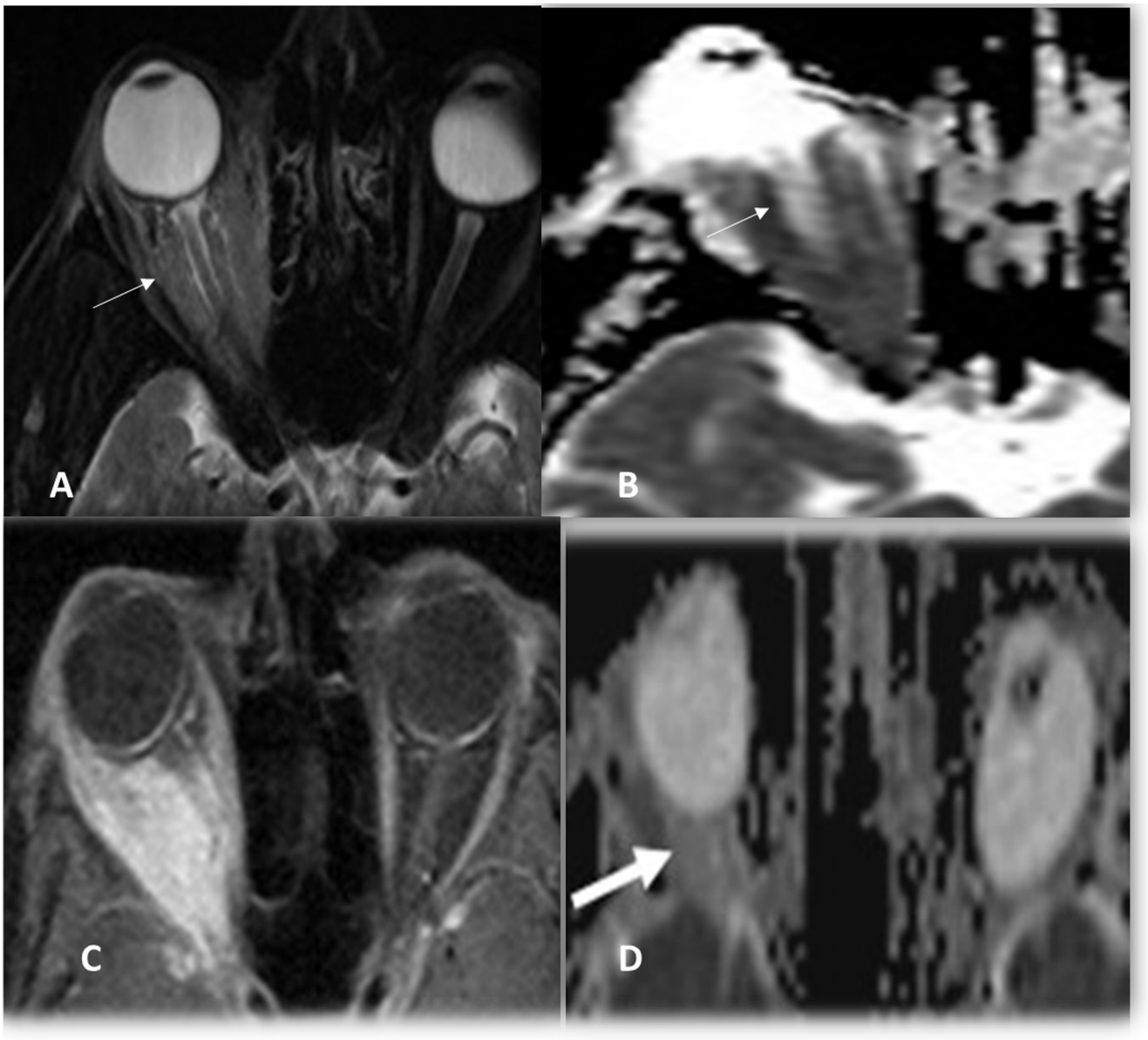


**Fig. 1.** A, B: Marginal zone lymphoma, fat suppressed Axial T2WI and ADC image showed restricted pattern (ADC = $0.74 \times 10^{-3}$ $mm^2/s$) of the diffuse right orbital mass (thin white arrow) C,D: Orbital Inflammatory disease post contrast-enhanced fat suppressed Axial T1WI and ADC showed ill-defined retrobulbar fat infiltrative lesion with enlarged right lacrimal gland not responding to medical treatment (thick white arrow) with ADC value = $1.42 \times 10^{-3}$ $mm^2/s$.

negative predictive value 88.9%. The ROC curve for the predictability of differentiating a benign from malignant diffuse orbital mass resulted in 88% validity (Fig. 4).

## 4. Discussion

In the present study, we utilized DW-MRI sequences adding ADC quantitative values to the standard MRI protocol in order to reveal the utility of this coefficient for the differential diagnosis of diffuse orbital mass.

This is a unique study that highlight the role and validity of ADC values derived by DW- MRI investigation to predict the diagnosis of diffuse orbital masses including all types of lesions with a confirmed diagnosis based on histopathological exam. Others studies of diffuse orbital mass using DW-MRI are based on small samples or a presumptive diagnosis [3].

Diffuse orbital mass refers to a large group of different lesions that are diagnosed mainly on the clinical presentation and response to treatment with some input from CT scan and MRI [11–16]. These lesions can be challenging to diagnose and treat and present with the risk of vision loss. Hence, ancillary exams may improve the pre-surgical diagnosis.

The outcomes of the current study showed clear differences between malignant and benign lesions. The malignant orbital tumors had significantly lower ADC values compared to benign lesions, confirming previous observations of malignant orbital lesions [1,3,9,10] and malignant tumors elsewhere in the body [17,18].

Based on our analysis, an ADC value of $0.8 \times 10^{(-3)}$ $mm^{(2)}$ $s^{(-1)}$ can be established as a threshold value for differentiating malignant from benign orbital mass. Hence, the ADC value can be considered a biomarker to differentiate malign and benign tumors [8].

In the present study we also found a significantly lower ADC value in lymphoma compared to other proliferative lesions. Lymphomas have the lowest ADC values compared to all other lymphoproliferative lesions such as Castleman disease, leukemia, atypical lymphoid hyperplasia and benign lymphoid hyperplasia. Additionally, ADC values in

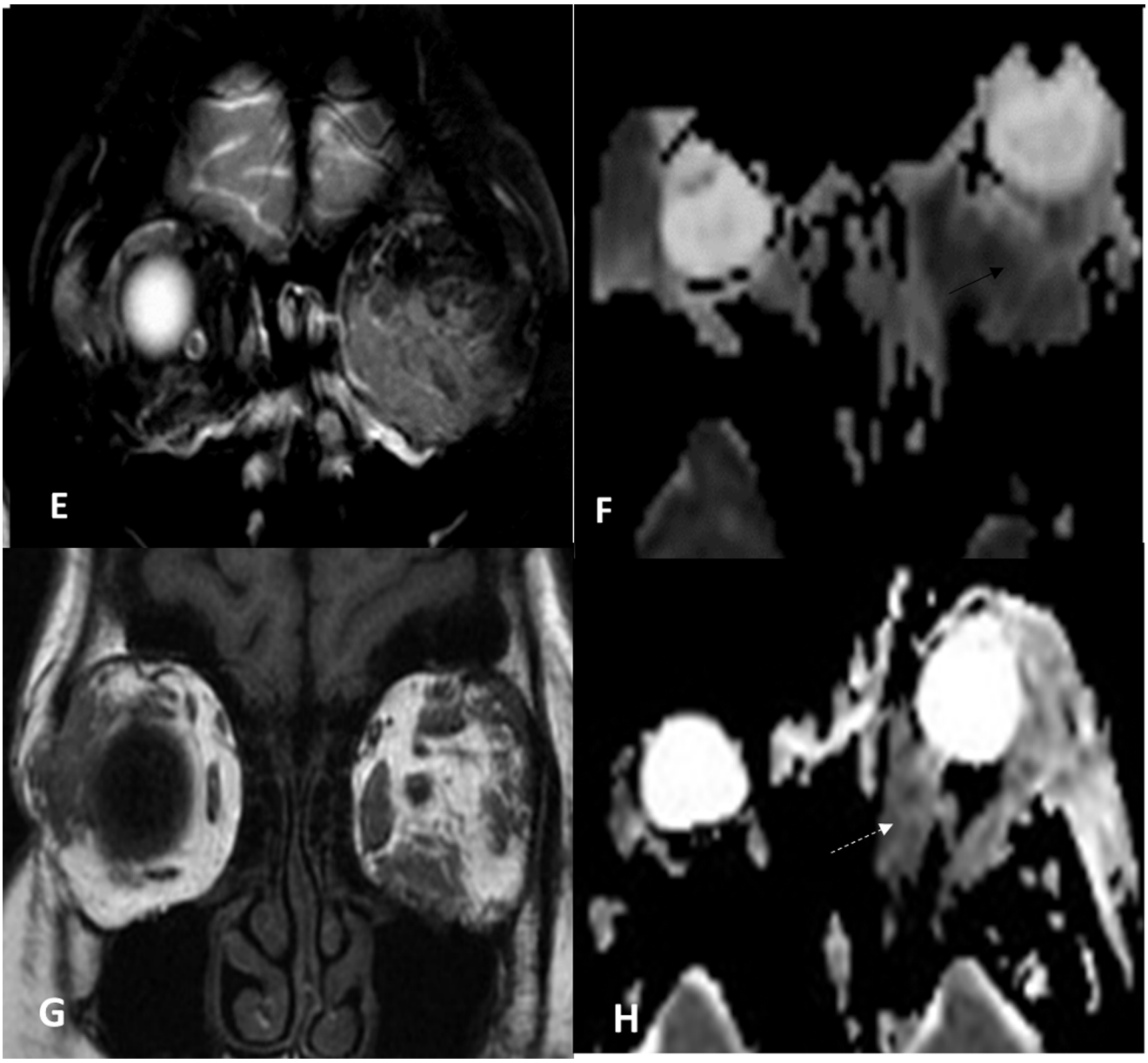


**Fig. 2.** E,F Castleman's Disease, Plasma cell type plus mixed type – coronal fat suppressed T2WI and ADC images showing diffuse infiltrative pattern of the intermuscular orbital fat (thin white arrow) ADC = $0.78 \times 10^{-3}$ sec/mm$^2$ . G,H: Angiolymphoid Hyperplasia with Eosinophilia – coronal T1 non fat suppression, axial ADC image shows bilaterality of the lesions with focal Infiltrative pattern of the muscle and surrounding fat with lacrimal gland involvement (white dotted arrow) with ADC value = $1.25 \times 10^{-3}$).

**Table 1**
Apparent diffusion coefficient (ADC) value (X $10^{-3}$ mm$^2$/s) in 39 diffuse orbital masses.

| | Number | Apparent diffusion coefficient ADC | | | | Validation |
|---|---|---|---|---|---|---|
| | | Median | 25% quartile | Minimum | Maximum | |
| Benign | 22 | 1.19 | 0.73 | 0.5 | 1.95 | M-W *U* test p 0.001 |
| Premalignant | 2 | 0.83 | 0.7 | 0.7 | 0.92 | |
| Malignant | 15 | 0.58 | 0.48 | 0.45 | 0.72 | |
| Lymphomas | 11 | 0.51 | 0.48 | 0.45 | 0.60 | M-W *U* test p = 0.02 |
| Others lymphatic lesion | 7 | 0.9 | 0.7 | 0.5 | 1.72 | – |

lymphomatous lesions are significantly lower than tissue in the normal eye such as the optic nerve, vitreous body, extraocular muscles, lacrimal gland and other benign orbital lesions (eg. vascular tumors) [9]. Previous studies indicate that DW-MRI is highly sensitive and specific for differentiating lymphoma from inflammatory orbital conditions [1,8,10].

Previous studies of the prediction of orbital lymphoma suggested threshold values of ADC of $1.15 \times 10^{(-3)}$ mm$^{(2)}$/s [19], $1.0 \times 10^{(-3)}$ mm$^{(2)}$/sec [10], or $0.775 \times 10^{(-3)}$ mm$^2$/sec which are similar to our value[9]. The differences between our ADC threshold value and the values from previous studies are likely due to difference the study samples, difficulties in obtain satisfactory images or imaging artifact [8].

Differences in ADC values can be explained by cellularity, necrosis or perfusion [1]. Malignant tumors have hyper-cellularity and are constituted by cells with enlarged nuclei and reduced extracellular matrix resulting in more restricted diffusion with low signal intensity areas and low ADC values [1,3,9,10]. ADC values can be also affected

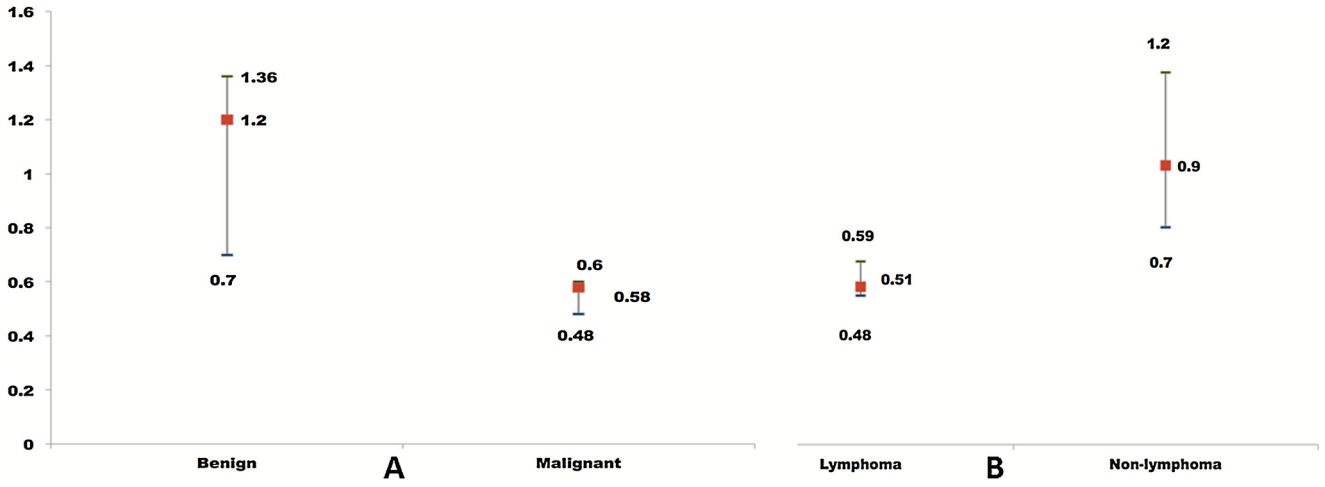


**Fig. 3.** A,B: A: Comparison of ADC values from DW-MRI of benign and malignant histopathology confirmed diffuse orbital lesions and B: ADC values of diffuse orbital lymphoma and other lymphoproliferative lesions (B).

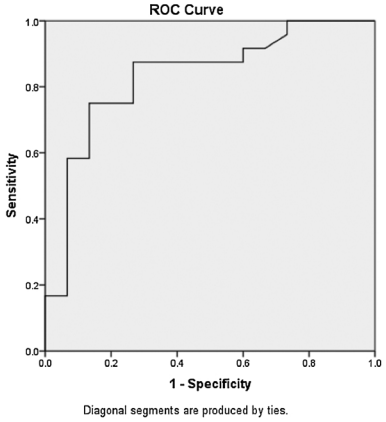


AUC = 0.832

| ADC | Benign | | Malignant |
|---|---|---|---|
| >0.83 | 16 | 2 | 18 |
| <0.83 | 8 | 13 | 21 |
| | 24 | 15 | 39 |

| | |
|---|---|
| Sensitivity | 66.7 |
| Specificity | 86.7 |
| False positive | 11.1 |
| False negatives | 38.1 |
| Positive predictive value | 88.9 |
| Negative predictive value | 61.9 |

AUC=Area under the curve; apparent diffusion coefficient (ADC) value in diffusion-weighted magnetic resonance imaging (DW-MRI)

**Fig. 4.** Area of receiver operating characteristic (ROC) curve (graphical plot of the sensitivity vs. 1–specificity) for using ADC values derived from DW MRI for cases with benign diffuse orbital mass.

by the presence of proteins and molecules in the extracellular space, increasing tissue viscosity, resulting in diffusion restriction [20–22]. Hence, low ADC values are due to restricted diffusion areas attributed to hyper-cellularity and higher nuclear:cytoplasmic ratios, which are characteristics generally present in malignant lesions. The interstitial changes in benign lesions would lead to an increased ADC value [23]. ADC is higher in benign and inflammatory lesions due to interstitial changes resulting from increased capillary permeability with fluids in the extracellular space and increased intracellular fraction of water rather than cellular infiltration [1,10,23].

The ADC threshold value in predicting a malignancy had high sensitivity (86.7%), with specificity of 66.9%, positive predictive value of 61.9% and negative predictive value of 88.9%. These outcomes are very similar to previous studies which reported sensitivities of 63%, 93% or 96% and specificities of 84%, 91% or 93% [9,10,19].

There major limitation of this study is the retrospective design. Hence, the ADC values should to be interpreted with caution. However, the restricted diffusion areas correlated well with increased cellularity, not all orbital malignancies were hypercellular and some benign lesions such as meningioma, benign fibrous histiocytoma, fibrocytoma, and neurofibroma can occasionally be hypercellular [10].

Diffuse orbital masses are rare, hence, samples for each sub-categories can be rare. For example, there were only two premalignant lesions in the current study, which could introduce statistical error while comparing subgroups. A multicenter study or a meta- analysis of cases series is recommended to confirm the ADC values from DW-MRI in the subgroups from this study. Another limitation is linked to technical (imaging) artifacts. Application of strong gradients produces a magnetic susceptibility artifact, which is most pronounced at interfaces between air, bone, and soft tissue. Hence, lesions that are close to the orbital apex, interfacing sphenoid bone and sphenoid sinus are notorious for causing susceptibility artifacts and the ADC value can be inaccurate [24]. Hence, careful interpretation is required while interpreting lesions in this region. Although we have often noted some anatomic distortion in the orbit due to these effects, our images were adequate for evaluation.

The advantages of the current study include the confirmation that ADC DW-MRI value may be very useful for predicting malignancy in diffuse orbital mass and for differentiating lymphoma from other lymphoproliferative lesions with high sensitivity, negative predictive value and accuracy. This outcome indicates an acceptable diagnosis to proceed with treatment without orbital biopsy when the location of the tumor or patient conditions are unfavorable.

Predicting diagnosis through a noninvasive method instead of a therapeutic trial is always beneficial for the caregiver and patient. Advances in imaging techniques have enabled the use of DW-MRI in diagnosing diffuse orbital mass with minimal cost. [1,25,26] Continued efforts to improve DW-MRI techniques could make this tool even more useful for noninvasive diagnosis of diffuse orbital masses.

## Conflict of interest

Authors have no conflict of interest in relation to this manuscript.

## Funding

none

## References

[1] R. Kapur, A.R. Sepahdari, M.F. Mafee, et al., MR imaging of orbital inflammatory syndrome, orbital cellulitis, and orbital lymphoid lesions: the role of diffusion-weighted imaging, AJNR Am. J. Neuroradiol. 30 (1) (2009) 64–70.
[2] A.A. Abdel Razek, N.Y. Soliman, S. Elkhamary, M.K. Alsharaway, A. Tawfik, Role of diffusion-weighted MR imaging in cervical lymphadenopathy, Eur. Radiol. 16 (7) (2006) 1468–1477.
[3] A.A. Razek, S. Elkhamary, A. Mousa, Differentiation between benign and malignant orbital tumors at 3-T diffusion MR-imaging, Neuroradiology 53 (7) (2011) 517–522.
[4] M.N. Pakdaman, A.R. Sepahdari, S.M. Elkhamary, Orbital inflammatory disease: pictorial review and differential diagnosis, World J. Radiol. 6 (4) (2014) 106–115.
[5] S.M. Elkhamary, Lacrimal gland lesions: can addition of diffusion-weighted MR imaging improve diagnostic accuracy in characterization? Egypt. J. Radiol. Nucl. Med. 43 (2) (2012) 165–172.
[6] L. Tuntiyatorn, B. Nantawas, N. Sirachainan, N. Larbcharoensub, A. Visudtibhan, S. Hongeng, Apparent diffusion coefficients in evaluation of pediatric brain tumors, J. Med. Assoc. Thai. 96 (2) (2013) 178–184.
[7] K.F. Payne, J. Haq, J. Brown, S. Connor, The role of diffusion-weighted magnetic resonance imaging in the diagnosis, lymph node staging and assessment of treatment response of head and neck cancer, Int. J. Oral Maxillofac. Surg. 44 (1) (2015) 1–7.
[8] X.Q. Xu, H. Hu, H. Liu, et al., Benign and malignant orbital lymphoproliferative disorders: differentiating using multiparametric MRI at 3.0T, J. Magn. Reson. Imag.: JMRI 45 (1) (2017) 167–176.
[9] L.S. Politi, R. Forghani, C. Godi, et al., Ocular adnexal lymphoma: diffusion-weighted mr imaging for differential diagnosis and therapeutic monitoring, Radiology 256 (2) (2010) 565–574.
[10] A.R. Sepahdari, V.K. Aakalu, P. Setabutr, M. Shiehmorteza, J.H. Naheedy, M.F. Mafee, Indeterminate orbital masses: restricted diffusion at MR imaging with echo-planar diffusion-weighted imaging predicts malignancy, Radiology 256 (2) (2010) 554–564.
[11] J. Yan, Z. Wu, Y. Li, The differentiation of idiopathic inflammatory pseudotumor from lymphoid tumors of orbit: analysis of 319 cases, Orbit 23 (4) (2004) 245–254.
[12] S. Westacott, A. Garner, I.F. Moseley, J.E. Wright, Orbital lymphoma versus reactive lymphoid hyperplasia: an analysis of the use of computed tomography in differential diagnosis, Br. J. Ophthalmol. 75 (12) (1991) 722–725.
[13] A.R. sepahdari, L.S. Politi, V.K. Aakalu, et al., Diffusion-weighted imaging of orbital masses: multi-institutional data support a 2-ADC threshold model to categorize lesions as benign, malignant, or indeterminate, AJNR Am. J. Neuroradiol. 35 (2014) 170–175.
[14] D.E. Meltzer, Orbital imaging: a pattern-based approach, Radiol. Clin. North Am. 53 (1) (2015) 37–80.
[15] S.W. Atlas, L.T. Bilaniuk, R.A. Zimmerman, D.B. Hackney, H.I. Goldberg, R.I. Grossman, Orbit: initial experience with surface coil spin-echo MR imaging at 1.5 T, Radiology 164 (2) (1987) 501–509.
[16] G. Akansel, L. Hendrix, B.A. Erickson, et al., MRI patterns in orbital malignant lymphoma and atypical lymphocytic infiltrates, Eur. J. Radiol. 53 (2) (2005) 175–181.
[17] A. Abdel Razek, A. Mossad, M. Ghonim, Role of diffusion-weighted MR imaging in assessing malignant versus benign skull-base lesions, La Radiol. Med. 116 (1) (2011) 125–132.
[18] J. Wang, S. Takashima, F. Takayama, et al., Head and neck lesions: characterization with diffusion-weighted echo-planar MR imaging, Radiology 220 (3) (2001) 621–630.
[19] A. Razek, N. Nada, M. Ghaniem, S. Elkhamary, Assessment of soft tissue tumours of the extremities with diffusion echoplanar MR imaging, La Radiol. Med. 117 (1) (2012) 96–101.
[20] D.A. Rusakov, D.M. Kullmann, Geometric and viscous components of the tortuosity of the extracellular space in the brain, Proc. Natl. Acad. Sci. U. S. A. 95 (15) (1998) 8975–8980.
[21] M.C. Mabray, R.F. Barajas Jr., S. Cha, Modern brain tumor imaging, Brain Tumor Res. Treat. 3 (1) (2015) 8–23.
[22] F.M. Costa, E.C. Ferreira, E.M. Vianna, Diffusion-weighted magnetic resonance imaging for the evaluation of musculoskeletal tumors, Magn. Reson. Imaging Clin. N. Am. 19 (1) (2011) 159–180.
[23] J. Liang, H. Lv, Q. Liu, H. Li, J. Wang, E. Cui, Role of diffusion-weighted magnetic resonance imaging and apparent diffusion coefficient values in the detection of gastric carcinoma, Int. J. Clin. Exp. Med. 8 (9) (2015) 15639–15647.
[24] M.F. Mafee, M. Rapoport, A. Karimi, S.A. Ansari, J. Shah, Orbital and ocular imaging using 3- and 1.5-T MR imaging systems, Neuroimaging Clin. N. Am. 15 (1) (2005) 1–21.
[25] M.F. Mafee, Y. Inoue, R.F. Mafee, Ocular and orbital imaging, Neuroimaging Clin. N. Am. 6 (2) (1996) 291–318.
[26] A.A. Abdel Razek, G. Gaballa, G. Elhawarey, A.S. Megahed, M. Hafez, N. Nada, Characterization of pediatric head and neck masses with diffusion-weighted MR imaging, Eur. Radiol. 19 (1) (2009) 201–208.